International Journal of Metallurgical Engineering 2013, 2(2): 142-148
DOI: 10.5923/j.ijmee.20130202.05

Microstructure, Deformation and Fracture Behavior of Cr-Mo-V Steels

C. Gupta[2,*], J. K. Chakravartty[1], S. Banerjee[1]

[1]Materials Group, Bhabha Atomic Research Centre, Trombay, Mumbai , 400086, India
[2]On Sabbatical as JSPS Post-Doctoral Fellow to 3D/4D Material Science Lab Toyohashi University of Technology, Japan

Abstract The paper reports the uniaxial deformation and fracture behavior of two Cr-Mo-V steels used for nuclear structural components. The two steels are – a new member of low alloy steel in the 3Cr-1Mo class and a plain tempered martensitic stainless steel containing 12% Cr. The microstructure investigations were carried out on the 3Cr-1Mo steel by establishing the continuous cooling transformation diagram using dilatometry complemented by optical microscopy studies. The nature of continuous cooling transformation diagram showed typical characteristics of bainitic transformation over wide range of cooling rates for the 3Cr-1Mo steel. The deformation behavior of the two steels were characterized using a series of tensile tests carried out in the temperature range 25 – 600°C and over a wide range of strain rate. The characteristic anomalies observed from the temperature and strain rate dependence of strength and ductility parameters obtained from the tensile tests provided indication to the presence of Dynamic strain aging (DSA) phenomenon in both steels. It was found that the embrittling features of DSA phenomenon was rather innocuously manifested in 3Cr-1Mo steel with bainitic structure as compared with the 12%Cr steel with tempered martensitic steel. The extent of reduction in fracture resistance of the tempered martensitic steel in the DSA regime was characterized in the J_{IC} format using high temperature fracture tests. The studies revealed that a reduction in fracture resistance in the DSA regime occurred primarily due to the presence of cracking instabilities during the fracture tests. The difference in the manifestations of DSA in the two steels was rationalized on the effectiveness of the interstitial impurities to interact with dislocations in the martensitic and bainitic microstructure.

Keywords Cr-Mo-V Steels, Dynamic Strain Aging, Bainite, Martensitic Steels Deformation, Fracture Toughness

1. Introduction

Ferritic steels are well known materials of construction of various structural components in nuclear reactors[1,2]. Reactor pressure vessels and reactor support structures in the PWR's and BWR's, heat transport piping and end fitting in PHWR's are some of the important examples of applications where ferritic steels have been employed as component materials. There exists a great concern over the influence of embrittlement phenomena on the ability of the material to discharge their functional duties during the lifetime of the critical components in use in reactors. This has grown a fertile area of research dealing with the influence of embrittlement due to thermal, irradiation and environmental sources on the components[1,2].

The presence of plastic instabilities is known to influence the performance of structural materials adversely[1,3]. These steels possess nano/ultrafine grained microstructures with excellent combinations of strength and ductility[3,4]. A related but distinctly different phenomenon is the Portevin Le Chatelier (PLC) effect, which also has been known to occur in structural steels. It was first reported by Le Chatelier in 1909 and subsequently by Portevin and Le Chatelier in 1924[3]. Estrin and Kubin[3,4] have classified the various types of plastic instabilities into those that are caused when the work hardening has been suppressed and those that result from strain rate softening. The Lüders band formation during the occurrence of yield point phenomena belongs to the former while the PLC phenomena to the latter. The PLC effect has been regarded as a particularly insidious manifestation of the dynamic strain aging (DSA) phenomena [3]. The physical origin of DSA phenomena is due to the dynamic interaction of diffusing solute atoms with moving dislocations[4,5]. The manifestation of DSA in several alloy systems such as Fe, Ti, Al, Au, Zr alloys has been studied[4-10]. These studies convey that despite the early knowledge and investigations into the occurrence of DSA, the manifestations of PLC depend on the alloy system undergoing DSA. As a result there is a sustained need for characterizing the manifestation of DSA in the either newly developed alloys destined for structural applications or in those materials being used structural components, where it has not been studied as yet. Further, the influence of the microstructure on the manifestations of DSA in ferritic steels has not received serious attention. Hence the scope of

* Corresponding author:
joy_gupta71@yahoo.co.in (C. Gupta)
Published online at http://journal.sapub.org/ijmee

investigations includes the study of relative manifestations of DSA in two different structural steels with nearly similar interstitial impurity content but with significant differences in alloy content and microstructure produced from $\gamma \rightarrow \alpha$ shear transformation in steels. Such a comparison is expected to elucidate the influence of microstructure on the on the extent of degradation of tensile and fracture properties due to presence of DSA in structural steels.

2. Experimental

The materials used for the investigations are a new member of 3Cr-1Mo class of low alloy steel and a plain 12Cr tempered martensitic steel. This 3Cr-1Mo type steel is a new generation nuclear reactor pressure vessel material with optimized composition to mitigate temper and irradiation embrittlement[1]. The AISI 403 steel is used for end fitting applications in pressurized heavy water reactor. The respective chemical compositions of the two steels are given in table 1. A deformation dilatometer Bahr DIL 805 was operated in the quenching mode for the dilatometry studies. Hollow tubular samples of outside diameter (O.D) 4.0 mm, 250µm thickness and 10 mm length were used for the tests. The sample was placed between two alumina rods, one of which was connected to a LVDT with less than 1µm resolution for measuring the change in length during the phase transformations. A thermocouple was spot welded to the O.D of the sample and it was inductively heated to the austenitic temperature. The heating rate of 100°C/min was employed for all tests for carrying the austenitising of the sample at 1100°C for 10 minutes. For the purpose dilatometry studies a series of samples were cooled over the cooling rate range 1075°C/min to 2.2°C/min. The sample change in length (ΔL) and temperature (T) were acquired online by a 16 bit DAQ during the entire heat-hold-cool cycle.

Table 1. Chemical composition of the steels in %wt

element	C	Cr	Mo	V	Mn	Ni
AISI 403	0.11	12.0	-	-	0.5	-
3Cr-1Mo type	0.15	3.0	0.7	0.28	0.4	0.7

The tensile tests were carried out using a floor model of instron make universal testing machine. Uni-axial tensile tests comprised of monotonic pull as well strain rate change tests over the temperature range 25 – 600°C. The tensile parameters of strength and ductility were derived from the digital data acquired during the tests. A three zone furnace was used to heat the sample, the temperature of which was monitored using a K type thermocouple attached to sample guage. The high temperature fracture tests were carried out in J_{IC} format using 1 inch thick fatigue pre-cracked compact tensile samples with a/W ratio of 0.6. The unloading compliance technique as well as DCPD technique was used for characterizing the fracture toughness as a function temperature. For the high temperature tests the crack length was monitored using both COD guage as well as using the direct current potential technique. The cracklength conversion from the measured potential drops was estimated from the Johnson's formula. A custom made furnace was made to accommodate the COD guage arms and DCPD current and potential leads inside the furnace. The electronics of the COD guage was air cooled.

3. Results and Discussion

The dilatometry studies on 3Cr-1Mo type steel yielded the temperature range of austenite transformation as a function of the prescribed cooling rates from the non-linear regions in the change in length with temperature plots. The transformation start and fininsh points plotted on the loci of the cooling curve in a semi-log temperature – time axis provided the the CCT diagram of the 3Cr-1Mo steel. The CCT diagram of the 3Cr-1Mo steel is shown in figure 1. It is clearly seen that a single bay in the transformation is seen to occur over a wide range of cooling rates. At slower cooling rates the austenite decomposition occurs at much higher tempertaure into two products with clear demarcated regions in the temperature – time space.

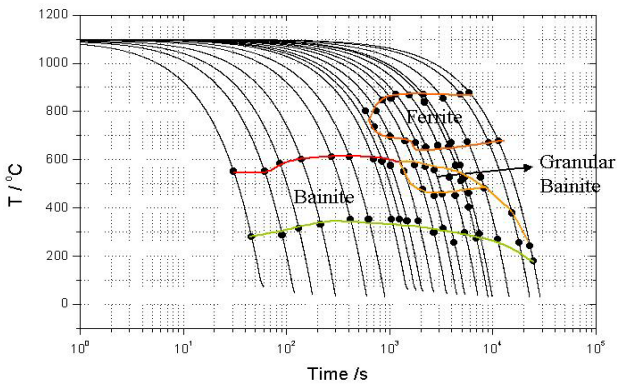

Figure 1. CCT diagram of the 3Cr-1Mo type steel

The optical microstructures of the samples exposed to selected cooling rates are shown in figure 2. At the faster cooling rates above 35°C/min the microstructure appears similar to the bainitic microstructure typically found in low alloy steels. Further the CCT diagram showing a single bay with transformation start temperatures to be insensitive to the cooling rates is typical of non-isothermal transformation characteristics of bainitic transformation seen in many steels[11]. At the slower cooling rates the optical microstructure shows that formation of pro-eutectoid ferrite (typical C- curve characteristics in the CCT diagram) followed by the formation of granular bainite. Within this region, the high resolution of the dilatometer detected multiple transitions below the bainite transformation start temperatures. Further investigations using interrupted quench studies need to be carried out establish the origin of these transitions. In this two phase region when the primary ferrite formation precedes the bainitic transformation, the

transformation start temperatures for the granular bainite decreases with slower cooling rate.

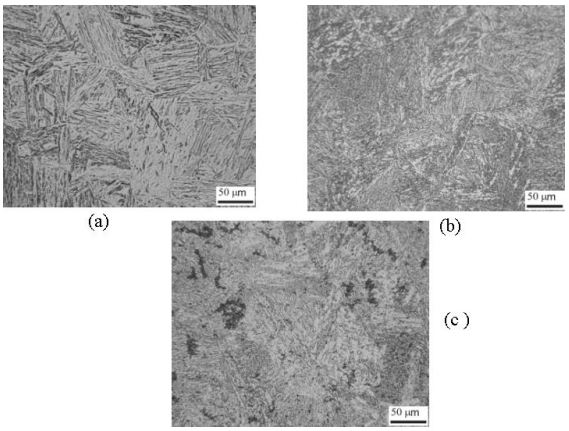

Figure 2. Optical microscopy of the dilatometry sample cooled at (a) 1080°C/min (b) 108°C/min (c) 43°C/min

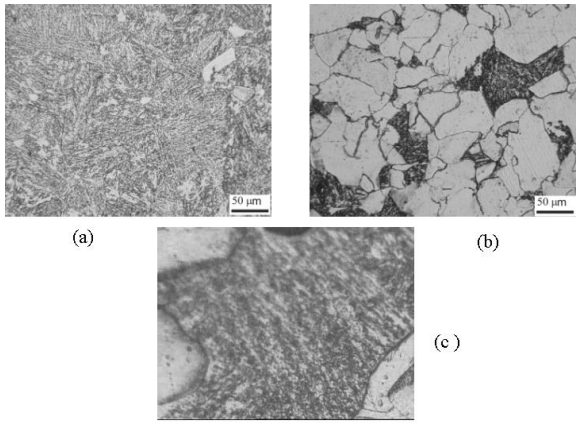

Figure 3. Optical microscopy of the dilatometry sample cooled at (a) 12°C/min (b) 6.6°C/min (c) A magnified picture granular bainite (500x)

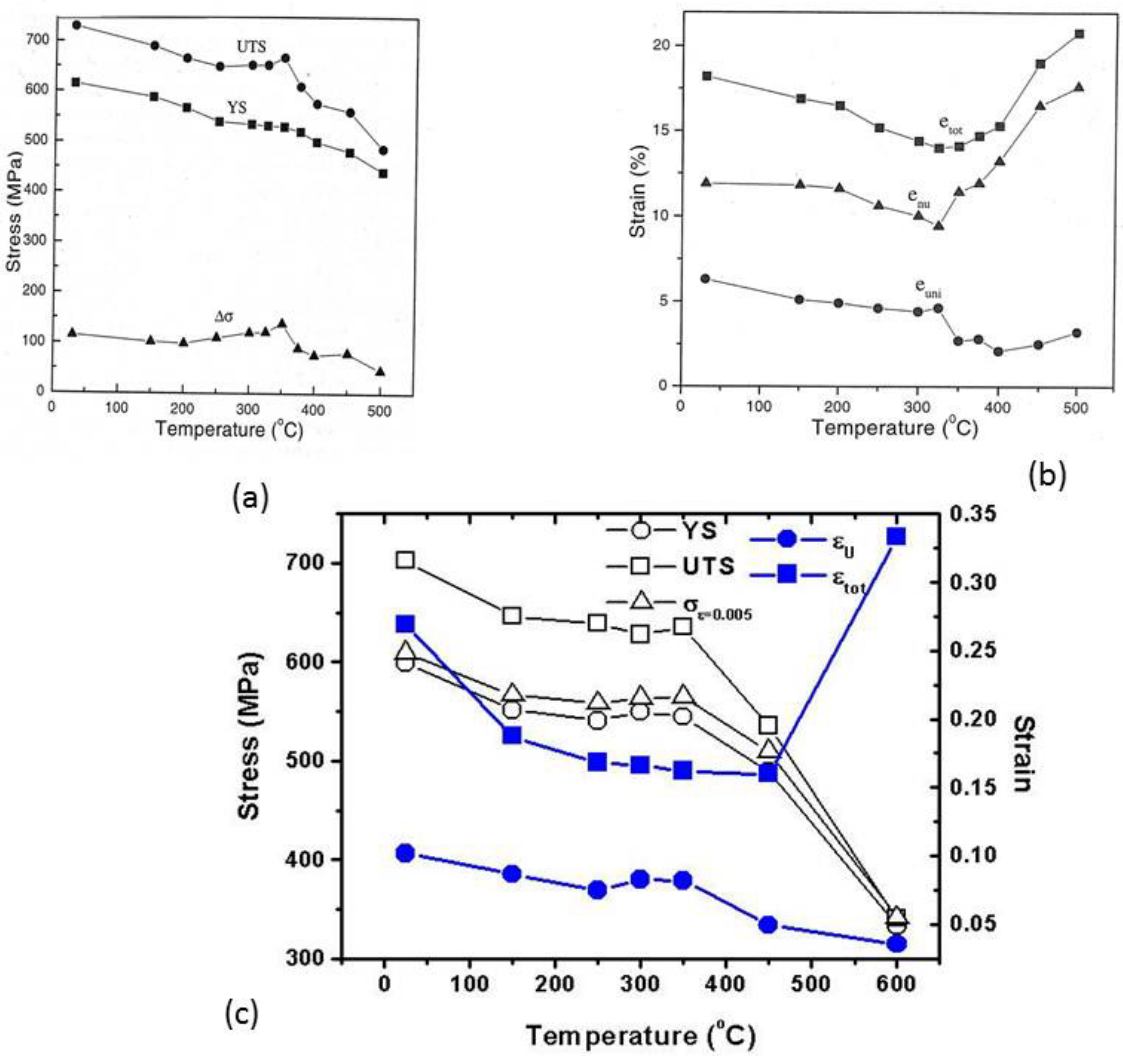

Figure 4. Variation of (a) UTS and YS (b) elongation (total, uniform and non-uniform) with test temperature for AISI 403. (c) Variation of UTS, YS, total and uniform elongation with temperature for 3Cr-1Mo type steel

Thus the overall characteristics of the CCT diagram and optical microscopy studies clearly establish that the dominant microstructure over a wide cooling rate is predominantly bainitic. This view is consistent with other microstructural studies on low alloy steels with similar alloy content for reactor pressure vessel applications[11]. The Bainite microstructure is a multi-component system with unique morphology of the bainitic ferrite having typical spatial orientation relationships with carbides, and austenite. TEM studies are envisaged to reveal these important microstructural characteristics in the bainitic structure of the new steel.

The tensile results for the two steels carried out are summarized in the figure 4. The temperature variation of strength and ductility parameters for the respective steels has been plotted. It is seen that for the AISI 403 there is a sharp increase in the tensile strength values accompanied by a decrease in ductility and stasis in the temperature dependence of yield strength in the range 250 – 400°C. In comparison it can be seen that the 3Cr-1Mo type steel displays no such increases in the tensile strength while undergoing similar reductions in the ductility parameters as AISI 403.

It is to be noted however that, within the temperature ranges 250 – 400°C the uniform ductility for the 3Cr-1Mo type steel improves before sharply reducing at higher temperatures. The total ductility contrastingly shows significant upswing at temperatures beyond 400°C for both steels. The occurrence of serrated flow occurred in both steels a typical example is shown in figure 5 for AISI 403. It needs to be mentioned however that the in-homogenous flow was quite damped in case of 3Cr-1Mo steel, with no clear delineation of critical strain.

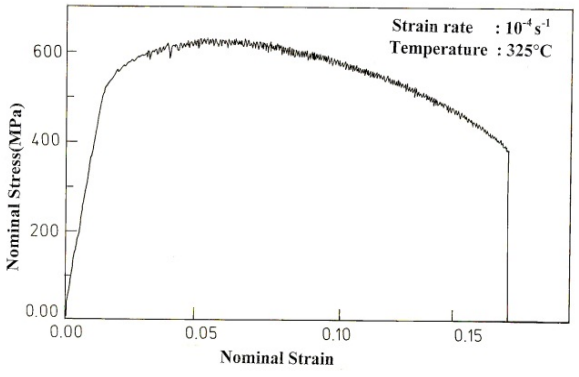

Figure 5. Stress-strain plot of AISI 403 showing serrated flow

The strain rate change tests carried out on both the steels enables characterization of the strain rate sensitivity as a function of temperature. The results are shown in figure 6. It can be clearly seen that both the steels show a reduction in the strain rate sensitivity towards negative values within the range 250 – 400°C.

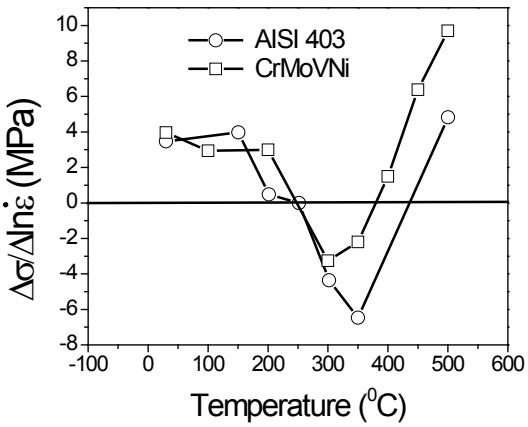

Figure 6. Plot comparing the strain rate sensitivity variation with temperature for the two steels

It is to be noted that the SRS values sharply decline to lower values for the AISI 403 steel than the 3Cr-1Mo type steel. The comparison of the tensile results between the two steels can summarized by the temperature dependence of the ratio $\frac{\sigma_{UTS}-\sigma_{YS}}{\sigma^{o}_{UTS}-\sigma^{o}_{YS}}$, which gives an idea of the extent of work hardening with the respect to that at the ambient conditions. The ductility parameters has been compared in terms of the ratio $\frac{\varepsilon^{1}_{Uni}}{\varepsilon^{2}_{Uni}}$, which gives an idea of the relative magnitudes of uniform ductility obtained from tensile tests carried out on AISI 403 and Cr-Mo-V steels. The plot is shown in the figure 7. It can be seen from the figure that within the DSA temperature regime, while there is dramatic increase in $\frac{\sigma_{UTS}-\sigma_{YS}}{\sigma^{o}_{UTS}-\sigma^{o}_{YS}}$ ratio to levels even greater than that at room temperature for AISI 403, the ratio for 3Cr-1Mo type steel shows a gradual decrease with increase in temperature.

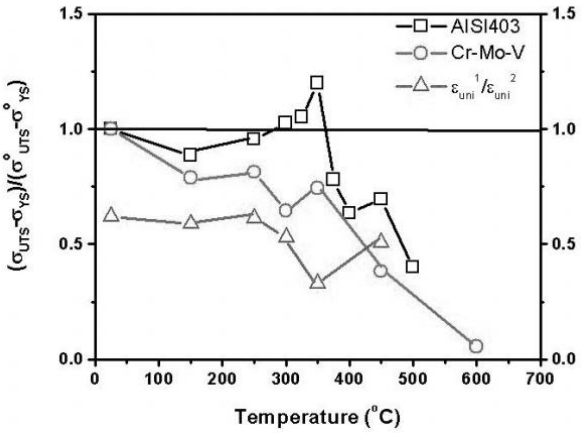

Figure 7. Comparing the temperature variation of the ratios pertaining to strength and ductility for the two steels

These trends imply that work hardening for AISI 403 with martensitic structure is significantly higher than that of 3Cr-1Mo type steel with baintic structure. A comparison of ductility ratio shows that it is less than unity at all temperatures, signifying that uniform elongation is smaller for the AISI 403 as compared with the 3Cr-1Mo type steel. It is to be noted that in the DSA temperature regime the ductility ratio decreases and reaches minimum at the temperature where the ratio $\frac{\sigma_{UTS} - \sigma_{YS}}{\sigma^{o}_{UTS} - \sigma^{o}_{YS}}$ for AISI 403 is the maximum. Thus the maximum difference in the ductility between the two steels occurs at the temperature where the work hardening for AISI 403 is the highest. As the uniform ductility for 3Cr-1Mo type steel remains relatively constant in the temperature range 250 – 350°C (Fig. 4(c)) it clearly implies that there has been greater embrittlement of AISI 403 as compared with 3Cr-1Mo type steel. These results bring out the fact that the AISI 403 steel have been more susceptible to extreme manifestations of DSA as compared with 3Cr-1Mo type steel. This has resulted in the greater deterioration of ductility in the temperature ranges where DSA was observed to occur for AISI 403 as compared with that of 3Cr-1Mo type steel.

The tensile results also show that the uniform elongation and total elongation curves diverge sharply beyond the DSA temperature range (figure 4). At the temperatures, where the SRS was found to be positive the contribution of non-uniform elongation to the total ductility of the steels is observed to be higher. This has been reported earlier in steels[12] and could be rationalized in the following way. It is well known that the attainment of tensile strength is controlled by both work hardening rate and strain rate hardening. However, only the latter remains active beyond UTS. As SRS controls the extent of strain rate hardening. The contribution of non-uniform elongation to the total elongation is directly related to its magnitude and sign of SRS. When it is negative, (i.e. serrated flow behavior) localization of deformation in the form propagative bands (eg. Lüders bands) and increase in work hardening promote development of local zones of damage, leading to decrease in both the ductility parameters. Beyond the DSA temperatures, a positive SRS would increase the strain rate hardening over that of work hardening rate. This is further exacerbated by processes such as dynamic recovery that promotes work softening[12]. While, these factors results in reducing the uniform elongation by inducing premature necking, they would be beneficial for non-uniform elongation, leading to the observed divergence between total and uniform elongation parameters as observed in figure 4.

In order to explore the extent of embrittlement of AISI 403 high temperature fracture toughness tests were carried out in the temperature range where serrations were observed in the steel. The strain rate - temperature domain of the occurrence of serrations in AISI 403 are shown in the figure 8, superimposed in which are the test conditions where the fracture toughness tests were carried out. The calculation of the effective crack tip strain rate was carried out from formula derived considering fully plastic solutions at crack tip[13] and was estimated as 3.8×10^{-3} s^{-1} for the applied pull rate shown in figure 8.

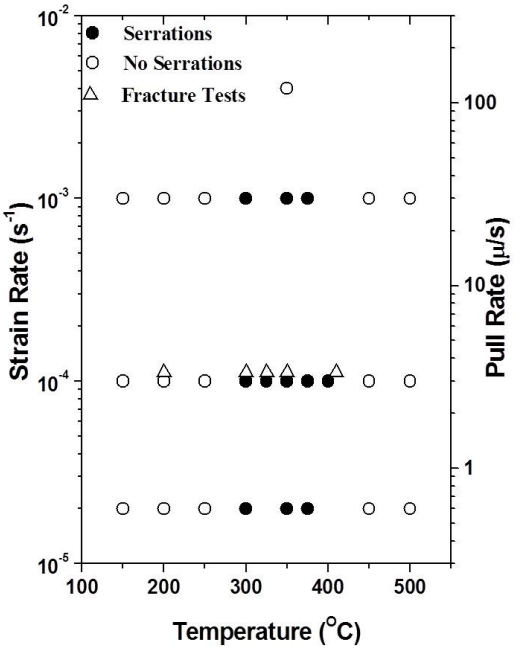

Figure 8. Plot showing the temperature – strain rate combinations where serrated flow (marked as filled circles) has been found in the tensile tests in AISI 403. The corresponding pull rates have also been shown

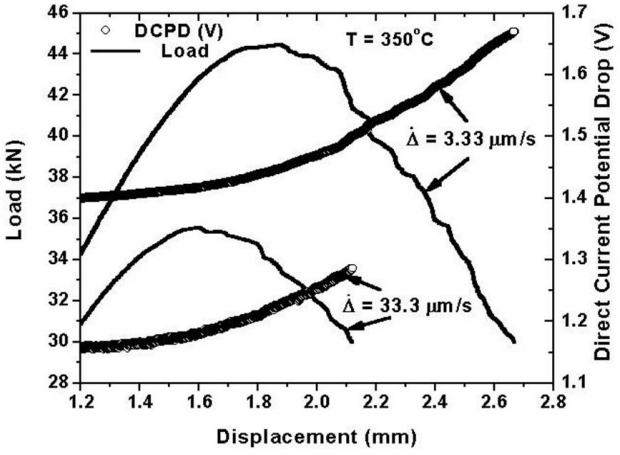

Figure 9. An enlarged portion of the load displacement plot obtained from the DCPD tests at 350°C and pull rate of 3.33 miron/s and 33.3 micron/s. The corresponding DCPD signal is also shown for each test

The load displacement curve and the corresponding DCPD signal is shown in figure 9 for two pull rates applied during the fracture toughness tests. It is clearly seen that the crack growth stage of the test (which occurs after the maximum load) shows perturbations in load and DCPD signal for the lower pull rate. This pull rate was within the DSA temperature – strain regime of AISI 403 where serrated flow was observed. On increasing the pull rates by a factor of 10, such perturbations in the load and DCPD signal was not observed. The estimation of the elastic plastic fracture

toughness parameters from the fracture test from the unloading compliance method and DCPD technique enabled the temperature variation of J_{IC} and dJ/da to characterized for AISI 403. Figure 10 shows the plot of J_{IC} and dJ/da with temperature. It is clearly seen that both the fracture toughness parameters decrease quite significantly in the temperature range 250 – 400°C.

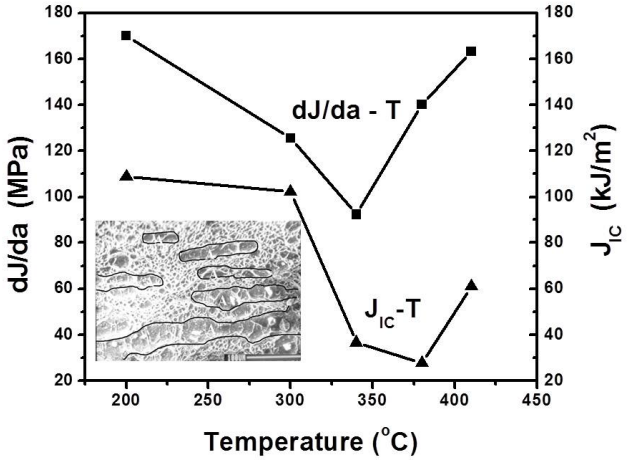

Figure 10. The evolution of fracture toughness in J_{IC} format and crack growth resistance in the dJ/da format over the temperature range 200°C to 425°C carried out using pull rate of 3.33 micron/s. Inset shows the SEM fractograph picture of the sample displaying the lowest fracture toughness value

The inset in the figure 10 shows the SEM picture of the fracture surface of the sample tested at the temperature corresponding to the lowest fracture toughness value. The SEM fractograph clearly shows the arrangement of under developed dimples interspersed between well developed dimpled areas. The width of these relatively flat areas in the SEM photograph is about 40μm.

It is therefore seen from the results obtained from the fracture toughness tests as well as fractographic examination that effect of DSA on fracture behaviour in AISI 403 results in embrittlement by way of reduction in the fracture parameters in terms of both initiation and propagation toughness. The fractographic observation clearly show evidences of flat featureless areas corroborating the 'jerky' load-displacement record obtained in the crack growth tests. The feature-less areas containing few ductile dimples are signatures of the occurrence of the crack jumps, because as pointed out by Mohan and Marschall[14], they result in rapid separation of the crack faces leaving less time for large number of voids to nucleate during the ductile crack growth.

The presence of these ductile cracking instabilities can also be associated with excessive machine compliance[14]. However in the multi pull rate crack growth tests the 'jerky' load-displacement record appeared only in the lower pull rate that gave an average crack tip strain rate within the DSA favorable strain rates. This rules out the influence on machine compliance. The second reason for these cracking has been attributed in ealrier studies[15,16] , primarily carried out on low carbon steels for piping applications, to DSA although the exact mechanism leading to periodic crack jumps has remained unclear.

A possible rationalization of the tensile test results, the appearance of cracking instability and its implication on the fracture parameters is now presented. Earlier investigations carried out by Mukherjee and Sellars[17] on Fe-Cr-C steels with tempered martensitic structure on a range of Cr contents (0.87% - 11.7%) attributed the dynamic strain aging to occur as a consequence of formation of Cr-C complexes, which enabled interstitial locking of dislocations upto 400°C. Thus the trends seen in AISI 403 are consistent with earlier investigations where the role of Cr has been unequivocally established. In the case of low alloy steels, to which the 3Cr-1Mo type steel belongs, studies have shown that they are susceptible to DSA due to interaction of dislocations with C and N[15-17]. The chemical nature of carbides in the tempered bainitic structure shows that they are Cr rich carbides[32] . As a result the elements such as Mn and Ni are free to form X-N or X-C complexes (X = Mn/Ni), thereby curtailing their migration to the dislocations. The formation of complexes of C and N with Mn are known to reduce the mobility of these interstitial atoms (i.e. C and N)[18]. Thus, as a consequence of the formation of Cr rich carbides, elements such as Ni/Mn could form complexes with C/N atoms, which may lead to a reduction in the effectiveness of dislocations pinning by these solutes.

The macroscopic effect of solutes pinning dislocations is to reduce the strain rate sensitivity. Louchet and Brechet[19,20] have studied theoretically the possible influences of strain rate sensitivity on toughness. They have argued that the strain rate sensitivity influences the action of crack tip relaxation process such as shielding and blunting[19]. Conditions that result in small values of strain rate sensitivity promote flow localization and retard the crack tip relaxation process, which can act as a driving force for crack extension by increasing the rate of stored elastic energy. Further, they have shown that in-homogenous deformation, such as the release of PLC bands at the crack tip lowers the stresses during their scanning time at the tip[20]. Considering the inferences from these studies[19,20] it may be proposed that in the fracture toughness tests carried out on AISI 403, with the release of PLC bands during DSA, the extent of plastification at the crack tip may be affected. With repeated release of these bands perturbations in the plastic zone size ahead of the tip may appear, which will impair the relaxation of local crack tip stresses. As a result an increase of the elastic strain energy rate would occur and provide the driving force for the crack extension in the form of jumps. The relationship between the plastic zone size and ability for crack tip shielding has been shown analytically by Chen et. al. where formation of reduced plastic zone size resulted in lower ability to relax the crack tip stresses[21]. As a result, the embrittling manifestations of DSA on the mechanical properties of AISI 403 steel are significantly increased.

4. Summary

The results in this work compares the manifestations of DSA in two steels with tempered martensitic and bainitic structures and attempts to show that phase transformation products also exert a non-trivial influence on the anomalies in tensile properties caused by the operation of the phenomena. Earlier studies where the austenite transformation products were ferrite, pearlite, martensite or a combination of them, chemistry control was found to be the controlling factor to reduce the influence of DSA on the tensile properties of the material. The results being reported in this work on the new generation low alloy steel show that chemistry control along with the presence of bainitic phase can be used to limit the full extent of manifestations of DSA on tensile properties. Further, as the potential for DSA in the material is pushed at higher temperatures, the ascendant influence of recovery processes (eg dynamic recovery) would suppress the embrittling features of the phenomena.

ACKNOWLEDGEMENTS

CG gratefully acknowledges Japan Society for Promotion of Science (JSPS) for the JSPS fellowship award and grant-in-aid for scientific research (No. 22.00384).

REFERENCES

[1] C. Gupta, Deformation and Fracture of Advanced Structural Steels: Effect of Dynamic Strain Aging, Ratcheting and Creep. Lambert Academic Publishers, Germany, 2012 pp. 20-35.

[2] K. L. Murty and C. S. Seok, JOM, Vol. 6 2001 p. 23.

[3] Y. Estrin and L. P. Kubin in: Continuum Models for Materials with Microstructure ed. H. B. Mühlhaus, John Wiley and Sons, Germany 1995 pp. 385-450.

[4] Y. Estrin and L. P. Kubin, Mat. Sci. Eng. Vol. A137 1991 p. 125.

[5] K. L. Murty J. Metals Vol. 16 1985 p.34.

[6] A. Gysler, G. Lutjering, and V. Gerold Acta. Metall. Vol. 22 1974 p.901.

[7] S. Banerjee and U. Naik, Acta. Mater. Vol 44, 1996 p.3997.

[8] P. Rodriguez, Bull. Mater. Sci. Vol 6 1984 p.653.

[9] E. Pink and A. Grinberg Mater. Sci. Eng Vol 51 1981 p.1.

[10] A. Van Den Beukel, Phys. Stat. Sol. (a) Vol 30, p.197.

[11] H. K. D. Bhadesia Bainite in Steels 2nd ed. IOM London 2001.

[12] W.P. Longo and R. E. Reed Hill, Scripta. Mat. Vol 6 1972 p.833.

[13] J. H. Yoon B. S. Lee, Y. J. oh and J. H. Hong, Int. Jour. Press. Vess. Pip Vol. 76 1999 p.150.

[14] R. Mohan and C. Marschall Acta. Mater. Vol 46 1998 p. 1933.

[15] B. Mukherjee, Nucl. Eng. Des. Vol. 111 1989 p. 63.

[16] J. W. Kim and I. S. Kim, Nucl. Eng. Des. Vol 172 p.49.

[17] T. Mukherjee and C. M. Sellars, Met. Trans Vol 3 1972 p. 953.

[18] C. C. Li and W. C. Leslie Met. TransA Vol. 9 1978 p.1765.

[19] Y. Brechet and F. Louchet, Acta. Metall. Mater. Vol 41 1993 p. 783.

[20] Y. Brechet and F. Louchet, Acta. Metall. Mater. Vol 41 1993 p. 793.

[21] J. Chen and S. Kitaoka, Int. Jour. Fract Vol 100 1999 p.307.